University of Reading

Upper tropospheric humidity

Book or Report Section

Accepted Version

John, V. O., Shi, L., Chung, E.-S., Allan, R. P. ORCID: https://orcid.org/0000-0003-0264-9447, Buehler, S. A. and Soden, B. J. (2020) Upper tropospheric humidity. In: Blunden, J. and Arndt, D. S. (eds.) State of the Climate in 2019. Bulletin of the American Meteorological Society, 101 (8). American Meteorological Society, S45-S46. doi: 10.1175/2020BAMSStateoftheClimate.1 Available at https://centaur.reading.ac.uk/92330/

It is advisable to refer to the publisher's version if you intend to cite from the work. See Guidance on citing.
Published version at: http://dx.doi.org/10.1175/2020BAMSStateoftheClimate.1
To link to this article DOI:
http://dx.doi.org/10.1175/2020BAMSStateoftheClimate.1

Publisher: American Meteorological Society

All outputs in CentAUR are protected by Intellectual Property Rights law, including copyright law. Copyright and IPR is retained by the creators or other copyright holders. Terms and conditions for use of this material are defined in the End User Agreement.

www.reading.ac.uk/centaur

University of Reading

CentAUR

Central Archive at the University of Reading

Reading's research outputs online

2.d.3 Upper Tropospheric Humidity

V. O. John[1], L. Shi[2], E.-S. Chung[3], and R. P. Allan[4], S. A. Buehler[5], B. J. Soden[6]

[1]*EUMETSAT, Darmstadt, Germany*

[2]*NOAA/NCEI, Asheville, North Carolina, United States*

[3]*IBS Center for Climate Physics, Busan, South Korea*

[4]*University of Reading, Reading, United Kingdom*

[5]*Universität Hamburg, Hamburg, Germany*

[6]*RSMAS, University of Miami, Key Biscayne, Florida, United States*

The 2019 global-average upper tropospheric (relative) humidity (UTH) continued to stay close to 2001-2010 average (+0.20 %RH; Fig 2.d.3.1). This implies a continued moistening of the upper troposphere with warming. A near-zero decadal trend in the UTH indicates an increase in absolute (specific) humidity in line with the warming mid- and upper troposphere (about 0.2 K/decade as shown for example in Santer et al., 2017), and hence is consistent with a positive (amplifying) water vapor feedback (Chung et al. 2016). The water vapor feedback is determined mainly by the mid to upper troposphere (Allan et al., 1999; Held and Soden, 2000) because the radiative effect of water vapor is proportional to relative changes in water vapor (John and Soden, 2007) and not to the absolute amount.

During the first half of 2019 the anomalies were slightly below average (-0.07 %rh compared to 0.10 %rh in the second half) indicating weak El Niño-like conditions (intensified Hadley circulation leads to enhanced subsidence in dry zones (e.g., Tivig et al, 2020)). During the second half of the year the anomalies were generally above average, associated with ENSO-neutral conditions. There is broad agreement among the three available datasets (HIRS

infrared satellite [Shi and Bates, 2011], microwave satellite data [Chung et al., 2013], ERA5 reanalysis [Hersbach et al., 2020]) in the interannual variability despite their structural differences. During their common period, there is a correlation of 0.6 between the two satellite datasets and 0.5 between ERA5 and either of the satellite datasets. This provides confidence in the observed long-term behavior of UTH. The inter-satellite calibrated and bias corrected infrared and microwave satellite measurements sample a broad upper tropospheric region (roughly between 500 and 200 hPa, but this layer varies slightly depending upon the atmospheric humidity profile) two times per day, and infrared observations only sample clear-sky scenes (John et al., 2011). The ERA5 reanalysis is based on model runs constrained with in situ and satellite data including the HIRS and microwave radiances. ERA5 samples all regions every hour, but here only displayed at 400 hPa. The mean and standard deviation of the anomaly time series are -0.17±0.87, -0.01±0.66, and 0.00±0.34 %rh for the ERA5, HIRS, and microwave datasets, respectively. Compared to its previous version (ERA-Interim), the ERA5 time series shows improved consistency with the satellite datasets but displays anomalies more negative than HIRS or the microwave data (~-0.5 %RH) during the period 1993-2002..

Annual anomalies of UTH for 2019 are shown in Plate 2.1 and Online Fig 2.d.3.1 for the microwave and HIRS datasets, respectively. Positive anomalies in central and eastern Africa reflect above average precipitation and flooding events in those areas. Negative anomalies over southern Africa indicate the drought conditions there. The strong positive phase of Indian Ocean Dipole (IOD) can also clearly be seen in the anomalies. During the positive phase of IOD sea surface temperatures in the Indian Ocean near Africa's east coast are warmer than usual, while sea surface temperature in the waters north-west of Australia are comparatively cooler. These conditions lead to below average precipitation across Australia,

which is also reflected in the negative UTH anomalies over most of Australia. The close connection of UTH to convection makes it suitable for monitoring large-scale dynamics of the troposphere.

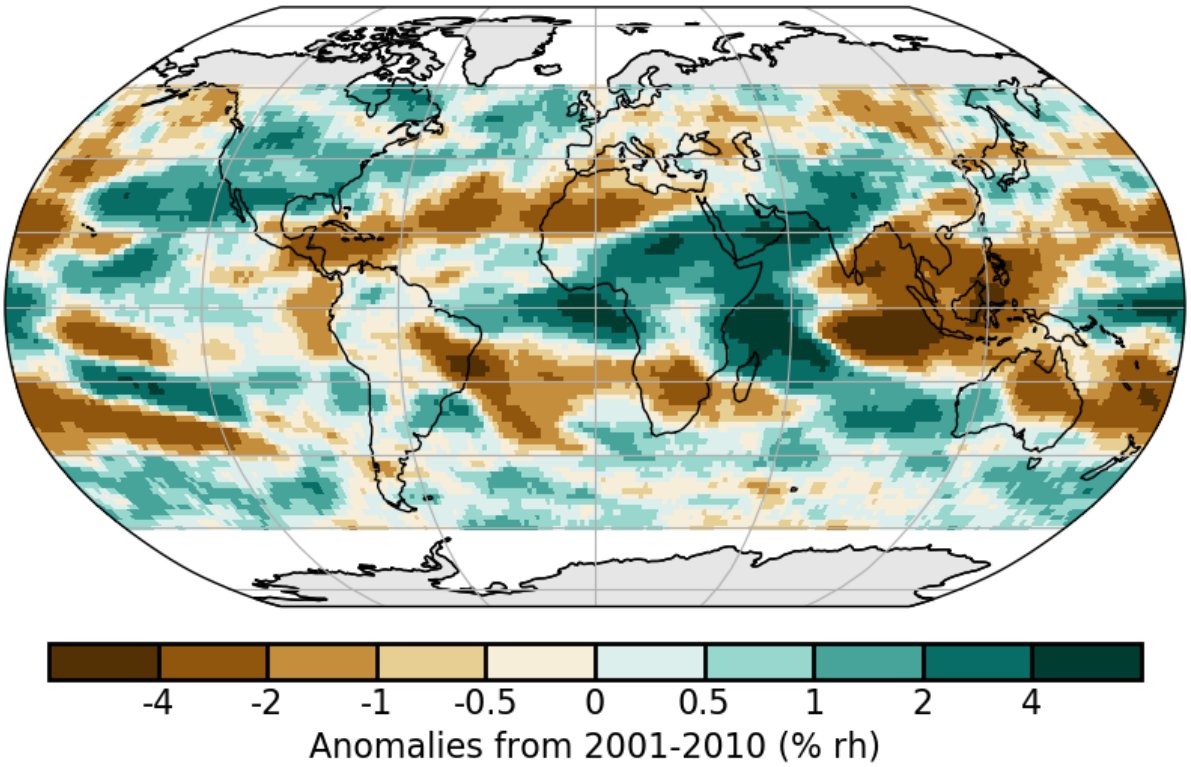

Plate 2.1: Annual average UTH anomaly map for 2019 relative to the 2001–2010 climatology based on the “all-sky” microwave-based UTH dataset.

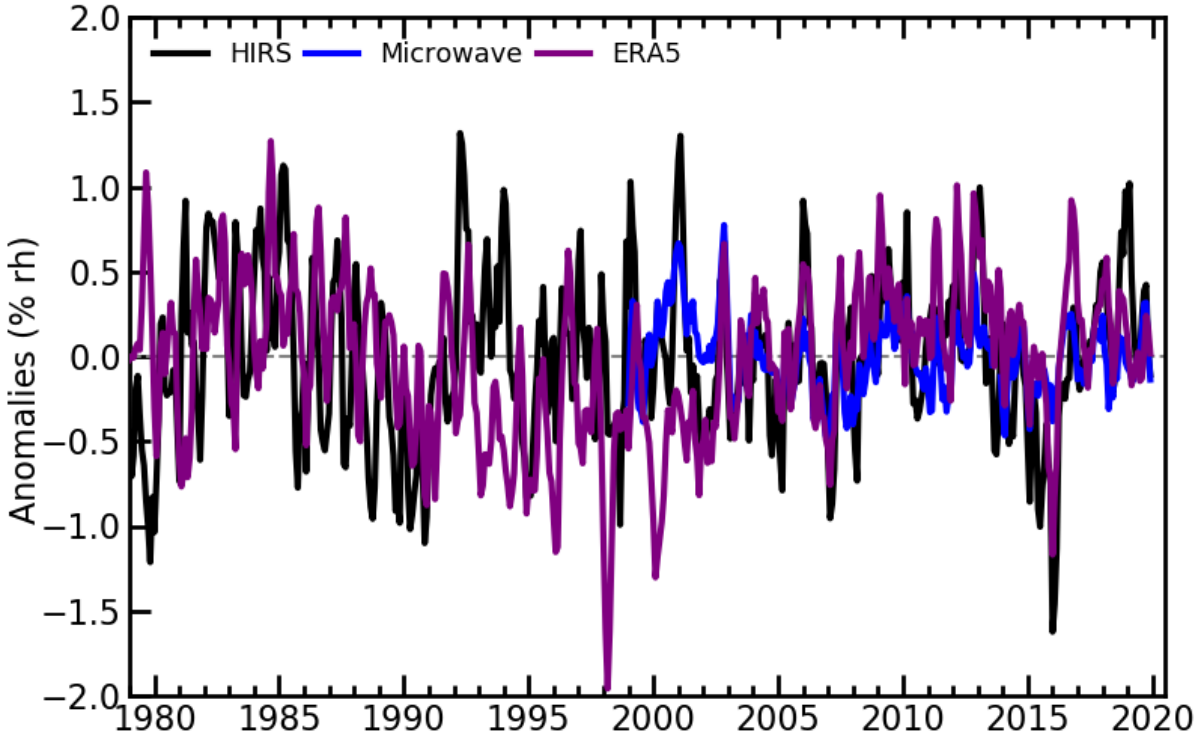

Fig 2.d.3.1 Global (60°S–60°N) average time series of upper tropospheric humidity anomalies using HIRS (black), microwave (blue), and ERA5 (purple) datasets. The anomalies are computed with respect to the 2001–2010 average, and the time series are smoothed to remove variability on time scales shorter than three months.

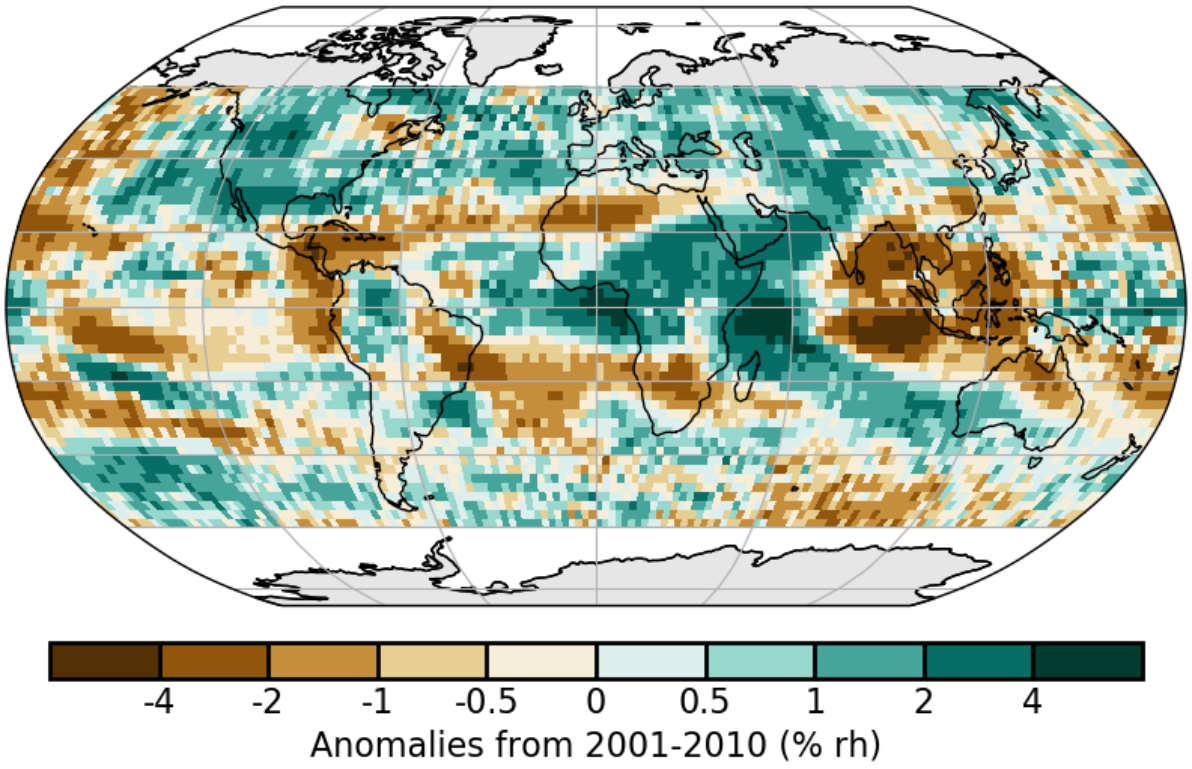

Online Fig 2.d.3.1 Annual average UTH anomaly map for 2019 relative to the 2001–2010 climatology based on the HIRS UTH dataset.

References:

Allan, R. P., K.P. Shine, A. Slingo and J.A. Pamment (1999), The dependence of clear-sky outgoing longwave radiation on surface temperature and relative humidity, Q. J. R. Meteorol. Soc., 125, 2103-2126, doi:10.1002/qj.49712555809

Chung, E., B. Soden, and V. O. John, 2013: Intercalibrating microwave satellite observations for monitoring long-term variations in upper- and midtropospheric water vapor. *J. Atmos. Oceanic Technol.*, **30**, 2303–2319, doi: 10.1175/JTECH-D-13-00001.1.

Chung, E.-S., B. J. Soden, X. Huang, L. Shi, and V. O. John, 2016: An assessment of the consistency between satellite measurements of upper tropospheric water vapor, *J. Geophys. Res. Atmos*., **121**, doi:10.1002/2015JD024496.

Held, I. M. and Soden, B. J., 2000: Water vapor feedback and global warming. *Annu. Rev. Energy Environ*., **25**:441–475.

Hersbach, H., et. al., 2020: The ERA5 Global Reanalysis. Quart. J. Roy. Meteor. Soc., submitted.

John, V. O. and B. J. Soden, 2007: Temperature and humidity biases in global climate models and their impact on climate feedbacks. *Geophys. Res. Lett*., **34**, L18704, doi:10.1029/2007GL030429.

John, V. O., G. Holl, R. P. Allan, S. A. Buehler, D. E. Parker, and B. J. Soden, 2011: Clear-sky biases in satellite infra-red estimates of upper tropospheric humidity and its trends, *J. Geophys. Res*., **116**, D14108, doi:10.1029/2010JD015355.

Santer, B.D., Solomon, S., Wentz, F.J. et al. Tropospheric Warming Over The Past Two Decades. Sci Rep 7, 2336 (2017). https://doi.org/10.1038/s41598-017-02520-7

Shi, L., and J. J. Bates, 2011: Three decades of intersatellite-calibrated high-resolution infrared radiation sounder upper tropospheric water vapor. J. *Geophys. Res*., **116**, D04108, doi:10.1029/2010JD014847.

Tivig, M., V. Grützun, V.O. John, and S.A. Buehler, 2020: Trends in Upper-Tropospheric Humidity: Expansion of the Subtropical Dry Zones?. J. Climate, 33, 2149–2161, https://doi.org/10.1175/JCLI-D-19-0046.1

Dataset URLs:

HIRS - https://data.nodc.noaa.gov/cgi-bin/iso?id=gov.noaa.ncdc:C00951

Microwave – Available on request

ERA5 – Climate Data Store